

**Neurological Modelling of the Vision System  
with Relevance to an Application for  
Improved Detection of Early Breast Cancer**

Thesis submitted for the degree of  
Doctor of Philosophy

By

Elysia Thornton-Benko BSc (Biol/Maths) MB BS (Hons)

Faculty of Science  
University of Technology, Sydney

January, 2005

*Engineers often view the eye as a kind of television camera with a certain bandwidth and dynamic range. Conversely, it is more natural for a biologist to see the visual system as an active synthesiser of the world we see. . . The visual system is dedicated to synthesising a world from inchoate patterns of light that reach the retina. Its ability to find order in a multitude of perceptual dimensions does, indeed, sometimes seem magical.*

Friedhoff & Kiely

Computer Graphics World 1990

## **Certificate of Authorship / Originality**

I certify that the work in this thesis has not previously been submitted for a degree nor has it been submitted as part of requirements for a degree except as fully acknowledged within the text.

I also certify that the thesis has been written by me. Any help that I have received in my research work and the preparation of the thesis itself has been acknowledged. In addition, I certify that all information sources and literature used are indicated in the thesis.

**Signature of Candidate**

*E. Thornton Benko*.....

## ACKNOWLEDGEMENTS

As with any PhD, a variety of people have contributed in some way whether it be providing necessary equipment, offering helpful suggestions, aiding with subject specific specialty knowledge. I feel honoured to have worked with many experienced people during this project and sincerely thank you all. Special mention must be made for the following:-

Professor Hung Nguyen, Principal Supervisor, provided the computer system, program and servo for the computer controlled polaroid motion in the experimental system and gave valuable information and references from his previous experience in microcalcification studies and computer based methods of assessment.

Associate Professor Loraine Holley, Co-Supervisor, provided important advice on experimental design and procedures, especially in regard to the methods for observers in the first and second series of observer trials. Her careful attention to project details was greatly appreciated.

Dr Arthur Hung as a Co-Supervisor externally, devoted considerable time assisting with computer programming for the model as well as assistance in the early years of the project regarding microcalcification characteristics and imaging. His statistical expertise was very valuable in the assessment of the experimental results.

The writer thanks all three supervisors for their patience and encouragement during the project especially towards the final stages while working full time as a hospital medical doctor.

The sets of unidentified mammograms for our tests were provided by Breast Screen NSW – Western Sydney, courtesy of Dr Warwick Lee, Deputy Chief Radiologist.

Mr Philip Ciddor, a Principal Research Officer at the National Measurement Laboratory, CSIRO, provided sets of polaroid sheets for use in the experimental system and also provided several reference papers on optical matters.

Dr Thomas Lee, Department of Statistics, University of Chicago, provided results from his program for segmentation for some of our microcalcification deposits in the initial stages of our study of calcifications.

Mr Paul Newman, a Project Manager with the National Health and Medical Research Council (NHMRC), Clinical Trials Unit, University of Sydney, provided helpful information on some practical aspects of trials in relation to the project.

Thanks are also due to the two groups of observers who gave their time generously for the sequences of experiments involved in the tests conducted in the Biomedical Laboratory at the University of Technology, Sydney (UTS). The cooperation from Mr Geoff Stockton in the Department of Physics (UTS) in obtaining the spectral data plots for the colour filters tested at several stages is appreciated. The writer also thanks Dr Peter Petocz of the School of Mathematical Sciences (UTS) for his interest in the experimental results and additional statistical calculations which may be avenues for future work.

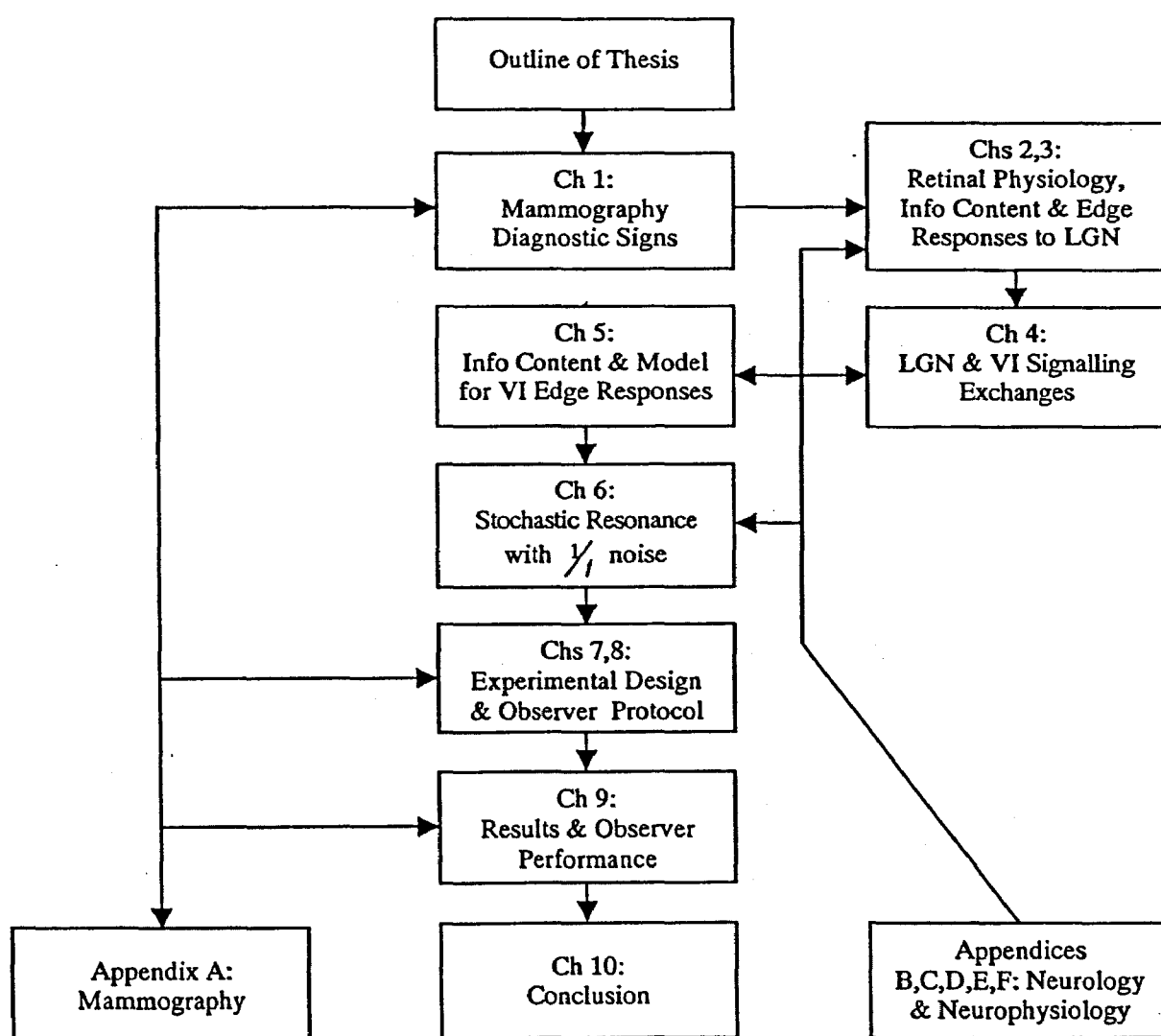
In addition much thanks goes to Fae Thornton for greatly assisting with the typing of the thesis as well as to Em. Professor Barry Thornton for his experience, support and guidance from the commencement of the project and especially later with regards to the mathematical modelling. I also am grateful to my husband Ivan Benko for his support and encouragement.

## TABLE OF CONTENTS

	Page
Abstract	1
Brief Outline of Thesis and its Significance	3
Chapter 1 Diagnostic Signs in Viewing Mammograms	13
Chapter 2 Basic Physiology of the Retina and its Edge Responses sent to the Lateral Geniculate Nucleus	22
Chapter 3 Spatial Frequency and Colour Information sent to the Lateral Geniculate Nucleus	44
Chapter 4 Processes at LGN, V1 and Signalling Interchanges	53
Chapter 5 A Functional Model for Edge Responses V1	70
Chapter 6 Possible Stochastic Resonance for $C_L$ and $C_D$ when Interaction Includes Coloured $1/f$ Noise	85
Chapter 7 Considerations for an Experimental Design	96
Chapter 8 Experimental Design, Observer Selection and Protocol	112
Chapter 9 Results of the Tests and Implications for Observer Performance	130
Chapter 10 Conclusion	139
Relationship of the Appendices in the Development of the Thesis	144
Appendix A Aspects of the Origin and Size Distribution of Breast Microcalcifications (Elysia Thornton-Benko and H. Nguyen, 1998)	146
Appendix B Neurons and Neural Signals Adapted from Adaptive Information Processing (Sampson 1976 and subsidiary references)	151

Appendix C	The Signal Pathways for Left and Right Eye and Further Information on M and P Channels	160
Appendix D	The Reticular formation and its Input	164
Appendix E	Neurophysical Comments on Extracts of Farley and Clark Experiments with a Neuron-like Net of Computer Elements	167
Appendix F	Directing and Focusing Attention to Locations in the Visual Field	170
References		171

### Structure and Flowchart



## LIST OF FIGURES AND ACKNOWLEDGEMENT OF SOURCES

Figures are listed below together with acknowledgement of sources (shown in brackets when obtained from the publications in the Reference List in the thesis. The sources are also acknowledged on the Figures themselves).

### Note Regarding Figures in the Chapters

There is a large number of figures in this thesis. To avoid discontinuity in reading the text, the figures are placed at the end of each chapter.

Brief Outline of Thesis	Page
Figure 1a, b      Details of mammograms showing microcalcifications (Lanyi, 1988)	8
Figure 2          Observed intensity shape resulting from $C_L$ and $C_D$ responses at the two edges of an object of finite width. Zero crossings marked with arrows	9
Figure 3a        Schematic diagram of the main visual pathways from retina to occipital cortex , showing the response profiles of receptive fields at various points along the pathway (positive to light spots, negative to dark spots). Also a separate diagram of the receptive fields of simple cells in the visual cortex: (a) line detector, (b) edge detector (Kulikowski, 1979)	10
Figure 3b        Magno and parvo paths from lateral geniculate nucleus (LGN) to V1 laminae (Milner and Goodale, 1995)	10
Figure 4          Primary retinotopic map (Cook, 1986)	11
Figure 5          Grossly simplified diagram of some major pathways within cortical area V1 (Crick, 1994)	12
 <b>Chapter 1</b>	
Figure 1.1       Schematic diagram of mature breast in axial section (Bassett et al, 1991)	17



		Page
Figure 1.2	Schematic diagram of ductal system (Adapted from Bassett et al, 1991)	18
Figure 1.3	Example of radiologist's reporting sheet, Breast Screening NSW – Western Sydney	19
Figure 1.4	Positioning for film-screening mammography (Bassett et al, 1991)	20
Figure 1.5	Criteria for selection for breast screening, World Health Organisation, (Thornton E., 2001)	21
<b>Chapter 2</b>		
Figure 2.1a	Structure of primate retina (Grusser and Grusser-Cornehls, 1987)	37
Figure 2.1b	Illustration of receptive field belonging to one ganglion cell (Gross M., 1994)	37
Figure 2.2a	Illustration of a small area of visual field showing excitatory and inhibitory region (Kent, 1981)	38
Figure 2.2b	On-centre and off-centre neuron spike responses for activation light spots shown (left) and the activation level in impulses per second of retinal neurons at light/dark edge (right) also shown is the response from a subsequent LGN on-centre contrast neuron (Grusser and Grusser-Cornehls, 19987)	38
Figure 2.3	Schematic diagram of main visual pathways from retina to cortex (Kulikowski, 1979)	39
Figure 2.4	Signalling pathways of retina from receptors to ganglions and optic nerve	40
Figure 2.5a	Computer plots of $C_L$ and $C_D$ differential equations for an edge with scale for comparison with Fig 2.5b	41
Figure 2.5b	Actual experimental data for $C_L$ (Baylor and Fuortes, 1970)	41
Figure 2.5c	Illustration of retinal physiology and extended retina with vertical pathway to ganglions. Lateral inhibition layer indicated (Cornsweet, 1970)	41

		Page
Figure 2.5d	Computer plots of $C_L$ (and $C_D$ ) for Figure 5a. Responses are repeated cyclically (not shown) corresponding to discharge and recharge of ganglions	42
Figure 2.6	Illustration of neuron pulses in axons giving an equivalent two-dimensional “byte” of information (spatial and temporal) (Kent, 1981)	43
<b>Chapter 3</b>		
Figure 3.1a	Distribution of rods and cones in the structure of the primate retina (Forgus, 1966)	49
Figure 3.1b	Retinal physiology (Grusser and Grusser-Cornehls, 1987)	49
Figure 3.1c	Spectral absorption of rods and cones in the human retina (Grusser and Grusser-Cornehls, 1987, adapted)	50
Figure 3.1d	Cone and rod visibility curves for absolute threshold as a function of wavelength (Forgus, 1966)	50
Figure 3.2a	Convergence pattern of retinal ganglion cells on a thalamic LGN cell (Kent, 1981)	51
Figure 3.2b	Convergence of thalamic LGN cells on to a simple field cell at the visual cortex (Kent, 1981)	51
Figure 3.3	Schematic view from underneath the brain of the primary visual system showing how messages from both eyes can be compared (Chesters, 1982)	52
<b>Chapter 4</b>		
Figure 4.1	Schematic diagram of connections between layers of the LGN and laminae of V1 (Geissler and Banks, 1995)	63
Figure 4.2	Illustration of the physiological component processes listed in the text.	64
Figure 4.3	Retinal on-centre and off-centre neuron activation (impulses per second) at an edge of light to dark illumination. Response for an LGN on-centre contrast neuron also shown (Grusser and Grusser-Cornehls, 1987)	65

		Page
Figure 4.4	Illustration of the different processing capacities low L to high H, of magno (M) and parvo (P) channels for spatially modulated (upper diagram) and temporally modulated stimuli (lower diagram) (Milner and Goodale, 1995, adapted)	65
Figure 4.5a	Basis of visual cortex hierarchical model of Hubel and Wiesel, (Martin, 2002)	66
Figure 4.5b	More recent alternative hierarchy with recurrent connections indicated (Martin, 2002)	66
Figure 4.6	A grossly simplified diagram showing some of the major pathways within cortical area V1. There are many sideways connections that are not shown in this diagram (Crick, 1994)	67
Figure 4.7	An algorithm representation for the convolution principle two sequences S(A) and S(G) to provide interaction of $C_L$ and $C_D$ components in V1 laminae (Cuenad and Durling, 1969)	68
Figure 4.8	(Redrawn from Zeki, 1975)	69
<b>Chapter 5</b>		
Figure 5.1	Representation of primary vision processes described in the text as both parallel and hierarchical and the result of the processes on $C_L$ shown at retina, LGN and V1	79
Figure 5.2	The “perceptual bus” hypothesis illustrating how parallel and hierarchical processes work together (Kent 1981)	80
Figure 5.3a	Illustration of experiment supporting spatial frequency selectivity of “tuning”, (Kent, 1981)	81
Figure 5.3b, 3c	Two possible methods of complex field cells “tuning” to specific spatial frequencies, (Kent, 1981)	82
Figure 5.4	LGN details with excitatory and inhibitory exchanges shown for magno and parvo pathways, (Bear et al, 1990)	83
Figure 5.5	Assured steps of spatial frequency channels as dependent across foveal	84

		Page
<b>Chapter 6</b>		
Figure 6.1	An illustrative example of a stochastic resonance for a subthreshold sinusoidal signal with Gaussian noise added, (Wiesenfeld and Moss, 1995)	94
Figure 6.2a	Orbital plot of $C_L$ and $C_D$ response (XY plane) and density of occurrences (vertical axis) with $1/f$ noise added to the interaction parameters in the L-V model in Chapter 5	95
Figure 6.2b	Orbital plot with density of occurrences for solutions of Stucki's example with $1/f$ noise added to just one parameter in one L-V differential equation, (Stucki, 1979)	95a
<b>Chapter 7</b>		
Figure 7.1	Principle of a method for generating $1/f$ type noise with respect to colour filters, polaroids and retinal receptors (adapted from Crandell, 1994)	103
Figure 7.2a	Illustration of the experimental system for providing $1/f$ noise based on the principles in Figure 7.1. Farley and Clark (1961) showed one-to-one correspondence for certain ranges of inputs	104
Figure 7.2b	The combination of motion of Polaroid P and polarization axes p of left and right eyepieces as shown with filters (blue, left; yellow, right) produces different temporal spectral inputs to each eye	105
Figure 7.3a	Magno and parvo pathways to cortical areas via the lateral geniculate nucleus. Parvocellular areas for colour and form are indicated and magnocellular interaction V3, V2 (adapted from NeuroScience, Bear et al, 1990)	106
Figure 7.3b	Illustration of receptive fields for colour specific neuron responses at retinal ganglions or LGN neurons (Grusser and Grusser-Cornehls, 1987)	107
Figure 7.3c	The four perceptual pathways from V1 to specialized visual areas of the prestriate cortex (Zeki, 1994)	108

		Page
Figure 7.4a	Human “brightness” function and optic tract activity as a function of frequency of intermittent light stimulation (Pinneo, 1971)	109
Figure 7.4b	Electrical activity of human optical tract during light adaptation and increasing and decreasing flicker frequencies (Pinneo, 1971)	110
Figure 7.5	Visual acuity as a function of retinal illuminance (Murch, 1973)	111
<b>Chapter 8</b>		
Figure 8.1a	Illustration of equipment configuration	124
Figure 8.1b	Preferred position of observed mammogram region in the equipment configuration to minimise any polarisation effects from the microcalcifications	124
Figure 8.1c	Photograph of servo mount with attached polaroid sheet	125
Figure 8.2	Computer screen control panel for dynamics of polaroid motion	126
Figure 8.3a	Transmission spectra of yellow filter sheet with eyepiece polariser sheet	127
Figure 8.3b	Transmission spectra of blue filter sheet with eyepiece polariser	128
Figure 8.4	Isophone (loudness versus frequency) curves of human hearing showing the auditory threshold curve (Grusser and Grusser-Cornehls, 1987)	129
<b>Chapter 9</b>	NIL	
<b>Chapter 10</b>	NIL	
	Relationship of the Appendices in the Development of the Thesis	144

	Page
<b>Appendix A</b>	
Figure A.1a, b	(a) Normal (N) and malignant (M) cells in contact and (b) normal and benign (B) cells. Dielectric zone formation reduces intercell communication between malignant cells (loss of contact inhibition) (Thornton and Nguyen, 1998) 150
<b>Appendix B</b>	
Figure B.1	Common features of neurons, (Sampson, 1976 for Figs B1-4) 157
Figure B.2	A form of chemical synapse 157
Figure B.3	Typical postsynaptic potentials 158
Figure B.4	An action potential 158
Figure B.5	The neuron and a schematic model of operation, (Windsor, 1988) 159
<b>Appendix C</b>	
Figure C.1	Difference in processing capacities of colour opponent, (CO) parvocellular and broad band (BB) magnocellular channels for both spatial and temporal frequencies (repeated from Figure 4, chapter 4) (Milner and Goodale, 1995) 163
<b>Appendix D</b>	
Figure D.1a	Connections of the reticular activating system and relationships to sensory functions (Kent, 1981) 165
Figure D.1b	Basic mechanisms of the control of attention involving the sensory functions and the reticular formation (Kent, 1981) 165
Figure D.1c	Sagittal section of brainstem showing location of reticular formation and related connections (McGraw Hill Encyclopaedia of Science and Technology, Vol. 9, 19770. 166
<b>Appendix E</b>	
Figure E.1	Computer simulation of a network of cells illustrating spatial clustering in the cortex of temporal inputs from a pattern, (Syme et al, 2002) 169

## **LIST OF TABLES**

<b>Table 1</b>	<b>Example of format for observations in Series B Test Results</b>	<b>120</b>
<b>Table 2</b>	<b>Results for observer preference in Series B 300 observations for “with noise”, “without noise” or “no change”</b>	<b>134</b>
<b>Table 3</b>	<b>Results of observers for “better”, “worse” or “no change” when noise was presented first or second in Series B observations</b>	<b>136</b>

## ABSTRACT

Detection and recognition of early signs of breast cancer when represented by cancer-related types of microcalcifications, are key requirements in breast screening mammography. Edge detection plays a vital role not only in observing detail in lesions with microcalcifications but also for the perception of often weakly defined stellate tumours. Mammograms are read at around 60 to 80 per hour.

We develop a neurological based functional model for edge responses of on-centre ( $C_L$ ) and off-centre ( $C_D$ ) groups of neurons in the early vision physiology, from the retina to the striate visual cortex V1. It is shown that the responses of the resulting differential equations at the retina and at V1 are of the Lotka-Volterra (LV) type. They display two important properties: consistency with the retinotopic property of early vision physiology and susceptibility to the  $1/f$  type noise for a stochastic resonance (SR) effect on the edge responses based on  $C_L$  and  $C_D$  interactions. Computer simulations of repeated cycles of the LV responses when  $1/f$  noise was incorporated into the interaction terms of the equations, showed an increased probability of occurrences of closely coupled small values of  $C_L$  and  $C_D$ . This indicated an underlying stochastic resonance effect. Such occurrences suggested a method for improved edge detection for “low observables” and improved detail in microcalcification regions in mammograms.

An experimental viewing system using a dynamic polaroid and eyepieces with colour filters was developed to provide  $1/f$  noise to test this hypothesis. It provided for the resulting  $C_L$  and  $C_D$  inputs from the left and right eye of an observer to interact in the V1 laminae. Using a set of 30 microcalcification region of interest images, tests were conducted in real-time readings with five observers, each at two different times. There was double blind randomisation of the sequence of images in addition to the order of presentation of “with” and “without noise”. The experience levels of the observers ranged from a low level working with technical images (not mammograms) to a high level experienced radiologist. An initial series of 300 observations using ratings of detail



quality (1 to 5) showed significance for an improved effect ( $p < 0.05$ ). A second series of 300 observations for a more stringent test with improved symmetrical experimental design of the equipment and alternative-forced-choice for observers to reduce subjectivity, showed a “trend to significance” ( $p < 0.1$ ). Observers with more experience had better performance in the tests ( $p \sim 0.07$ ). Intra-observer variability was consistently good compared with inter-observer results. A parameter in the L-V equations which is related to observer attention, coupled with a spatial search requirement, may be part of the inter-observer variability. The findings also have implications for the training of radiologists in reading mammograms in real-time screening. Recent developments in spectral properties of photonics materials may provide a simple implementation of the principles developed in the thesis.

## **Brief Outline of Thesis and its Significance**

The project deals with the early signs of breast cancer (details in lesions) with relevance to their visual detection in the breast screening process. Mammograms from screening are typically read at 60 to 80 per hour. Because only about 0.5% of these cases will have breast cancer, care and experience is required to find the often subtle indications of malignancy on a mammogram. Depending on the various data sources somewhere between 5% and 30% of women who do have breast cancer and have a mammogram are diagnosed as normal. Therefore any aid for detection of detail in real-time would be desirable. We develop a model for edge responses which allows us to test the ability of stochastic resonance to improve detection of stealthy edges and image details. Since microcalcifications are considered the earliest visible, non palpable features in nearly 25% of mammograms, attention will be given to them for our observer tests.. Also such deposits are easier to see than early stellate tumours by inexperienced observers used in our test for improvement of detail in lesions. Although only about 15% of cancers are detected solely on the basis of microcalcifications, other cases which are biopsied often exhibit microcalcifications which were not detected on initial screening. (This can relate to the extent of surgical margin required). Microcalcifications (Fig 1) are byproducts of a lesion and are “signs” in detection whereas masses need direct detection. The model developed for improving the visual detection by adding a type of noise can apply to both since both involve the need for acutance and acuity for recognition of edges and detail in real-time breast screening. In mammography, contrasts are inherently low due to small differences in the X-ray attenuation coefficients.

The thesis begins with an introduction to breast screening mammography and the nature and properties of microcalcifications which are used by radiologists when searching a mammogram. A good review of detection of microcalcifications is by Nishikawa (2002). We then proceed to the problem of actual edge detection. A seminal paper on the theory of edge detection by Marr & Hildreth (1980) developed a mathematical expression (not a model) to represent the “Mexican Hat” shaped response of an edge in the visual cortex

(Fig 2). They briefly commented on neurological and psychophysical implications but it was not intended as a physiological mechanism. Our project requires a model for edge responses in the early vision system. We develop it from the on-centre  $C_L$  and off-centre  $C_D$  neurons in early vision. The model allows us to investigate if our proposed addition of coloured  $1/f$  type noise might cause stochastic resonance with small objects such as microcalcifications close to the visual threshold. Such noise has correlations over most frequencies  $f$  in its power spectrum which declines as  $1/f$  and these characteristics can be of value regarding possible resonances for size and cluster distribution.

The primary visual pathway begins at the retina and involves the lateral geniculate nucleus (LGN) and the visual cortex V1. A greatly simplified illustration of the visual pathways is shown in Fig 3a (Kulikowski, 1979). The LGN is a small but very important part ( $\approx 1.5$  million cells) of the thalamus in the pathway for each eye. Retinal ganglions receive spatial information in the form of excitatory (“light”) and inhibitory (“dark”) signals and transmit this information via action potential spike pulses to the separate layers of the LGN. Each LGN relays signals to the visual cortex V1 but it also is involved with extensive signals back-projected from the cortex and associated neurological processes, not all of which are known in their exact functions.

The striate cortex V1 has six laminae due to many myelinated axons running roughly parallel to the cortical sheet, (Fig 3b). Its network of neurons performs extensive interactions of visual information originating from both eyes and sends rapid messages to many other parts of the brain.

The shape of the retinal image is conformally preserved in its general spatial relationships in the transmission from the retina to the LGN and on to the striate cortex. This is the primary “retinotopic” map of early vision illustrated in Fig 4 (Cook, 1986). At the visual cortex on-responses and off-responses interact by processes indicated in Fig 5 (Crick, 1994). The results of these interactions may be achieved in our model by a simple convolution process using the versatile properties of neurons. By using such processes

the cortical area can communicate its messages very rapidly because it is believed that it performs very few iterations before doing so. Therefore the usual concept of computations requiring many iterations probably does not apply (Crick, 1994). This is supported by the absence of extensive inhibitory neurons which would be needed for extensive computation.

Much of our knowledge of the neurological structure and properties of cell types in the vision system comes from the extensive work of Hubel and Wiesel in the 1960's and 70's (eg see Hubel and Wiesel, 1977). (Nobel Prize in Medicine awarded 1981). Their work is still the basis of much research in vision. The two main information pathways in the vision system are for the on-centre and off-centre neuron responses which are initially generated at the receptive fields of retinal neurons. This is an efficient method used by the vision system for eventual contrast detection in the visual cortex of the observer. The important on- and off-spatial response gradients determine the "zero crossings"(ie light  $\leftrightarrow$  dark) corresponding to the arrows in Fig 2 at the inflexions of the edge intensity response. A surprising theorem of Logan (1977) shows that this information at zero crossings contains all that is required to define the response. We utilise this fact and designate the respective information content of on-centre and off-centre groups of cells involved for edge transition from dark(D) to light(L) as  $C_L$  and  $C_D$ . These respond antagonistically in excitatory or inhibitory mode depending on the light or dark regions of the image component presented at the particular spatial retinal receptors which are associated with subsequent convergence of signals on to a particular retinal ganglion. Signals from groups of ganglions are then responsible for the coded image messages sent into the optic nerve channels to the LGN.

The two separated on- and off-pathways from the retinal ganglions undergo a division at the LGN into a magno (M, large cell) and parvo (P, small cell) path. There is also some individual "sharpening" of responses at the LGN in addition to psychophysical feedback from the reticular formation at the top of the brainstem via the inferior temporal cortex (ITC). By this stage the pathways carry spatio-temporal, size, and colour information as well as spatial frequency components of the image. Our experimental arrangement in

which  $1/f$  "coloured" noise is added, results in the effect being registered in the cortex V1 in liaison with the cortex region V4 (for any colour perception).

We use the visual system's development of "information content" from Information Theory to allow us to compare the spatial information of  $C_L$  and  $C_D$  at V1 and that which is input from the previous LGN level. The algebraic difference between results of processes at  $C_L$  and  $C_D$  for spatial gradient at LGN and V1 must be due to the processes for the result at V1. This yields a differential equation for each of  $C_L$  and  $C_D$  from which their spatial response at V1 can be formulated. The spatial gradients of  $C_L$  and  $C_D$  directly effect the intensity contrast for the actual perception by the observer at higher cortical levels.

We show that a class of Lotka-Volterra differential equations can describe the retinal ganglions output and that similar equations also arise in the V1 striate cortex where the on-centre and off-centre responses are interactively combined. This similar class of equations at both locations is supported by the known retinotopic property of early vision. We then suggest that a property of the L-V differential equations in regard to responses from the addition of  $1/f$  noise injected into the interaction process of our model at V1 can produce a type of selective stochastic resonance (SR) in the cortex to improve contrast. This arises as follows: the brain, and neurons generally, are noisy but this random noise does not affect normal vision. However, published research has shown that other classes of noise including  $1/f$  type noise, can produce resonance solutions to L-V equations. Our hypothesis is that in the physical system of our experiment, in which we can internally introduce ( $1/f$ ) noise to V1 of the observer, resonances in the on-responses and off-responses can occur for edges and associated details.

The results from 300 observations is an initial set of observations from two groups of observers indicate that the effect is present ( $p < 0.05$ ). In a subsequent second set of 300 observations with more stringent conditions the significance value was  $p < 0.1$ . Values

of  $p \sim 0.07$  occurred for observers who have had some experience in viewing detail in images (not necessarily mammograms). The probable reasons appear to be associated with observer-related parameters in the L-V equations. Implications for breast screening are discussed in relation to attention and search methods used by observers.

We note that a recent report (Kitajo et al, 2003) shows that random Gaussian noise introduced to only one eye during a periodic change in intensity of a patch area of illumination on a computer screen viewed by both eyes increased the observers' ability to detect the periodic change below the visual threshold compared with the eye without noise added. Although this indicates SR occurring in the cortex, it is not for improvement of edge detection which is quite a different neurological process which is not susceptible to Gaussian noise in our model, for stochastic resonance. Nevertheless it supports our approach of using signal interactions with  $1/f$  noise at the visual striate cortex.

Other applications of the system may include resolving identification uncertainties between some types of calcium deposits and pulmonary nodules in chest X-rays, as suggested to us by a senior radiologist who had participated in our experimental observations.

Forthcoming opportunities for other new technology from digital electronics and spectral properties of photonics materials hold promise for visual detection aids, based on the principles presented in the thesis.

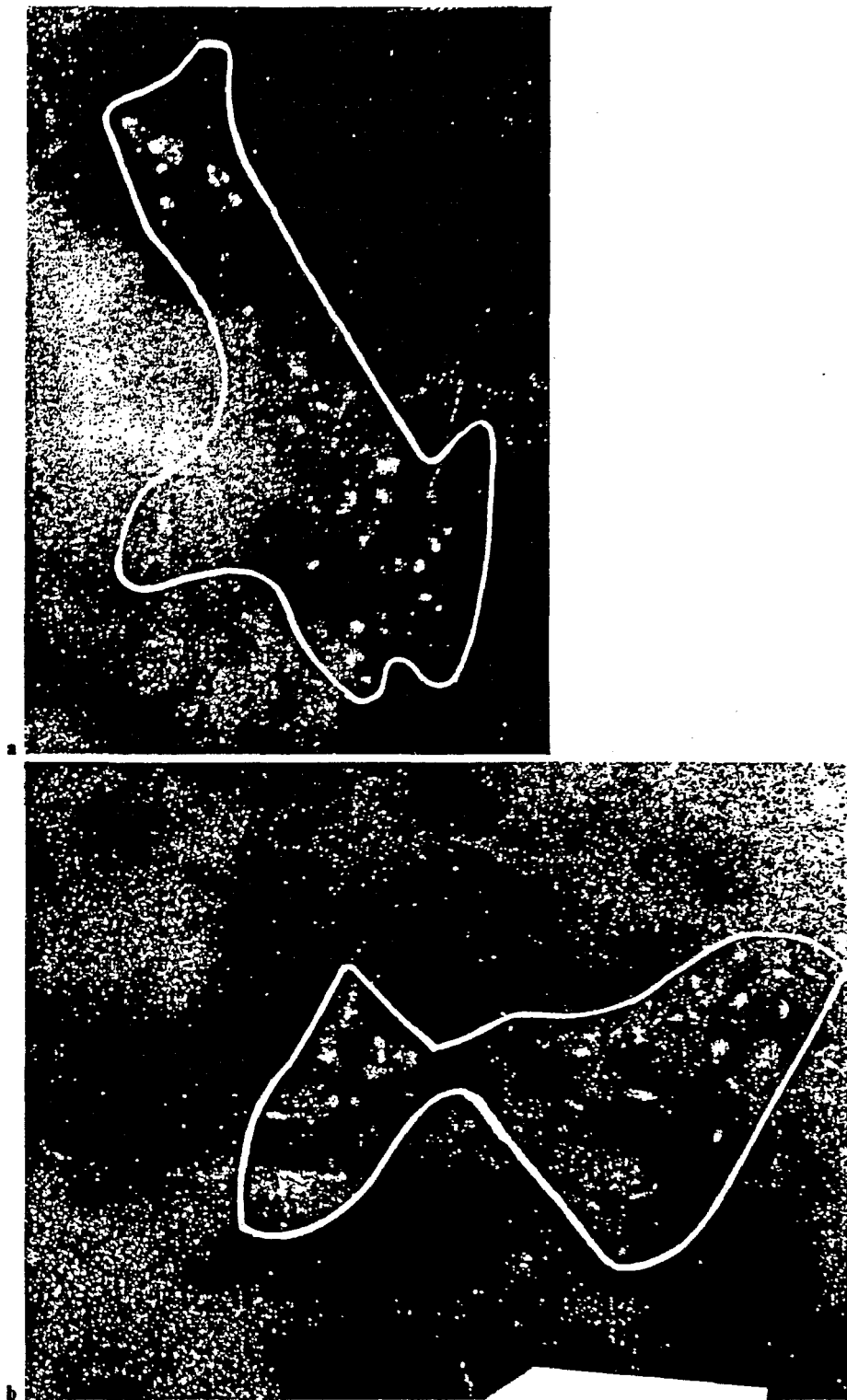


**Fig 1 a,b. (Lanyi, 1988)**

**Details of mammograms (5 X ).**

- a. Lateral view: faint cluster of polymorphous microcalcifications. The cluster shape is difficult to evaluate (bottle-shaped? Triangular?).**
- b. Craniocaudal view of the same area: the cluster is propeller – or butterfly-shaped**

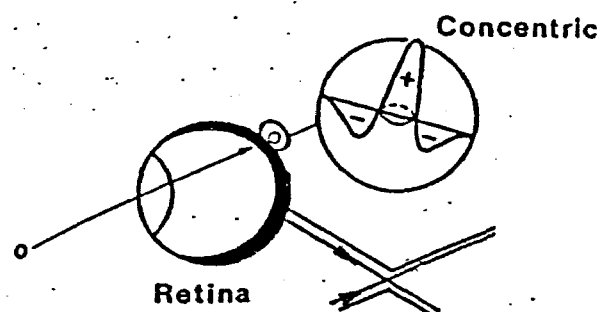
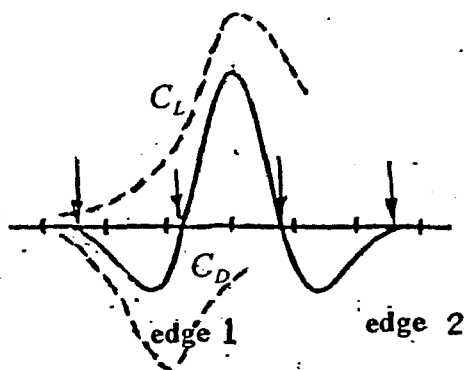
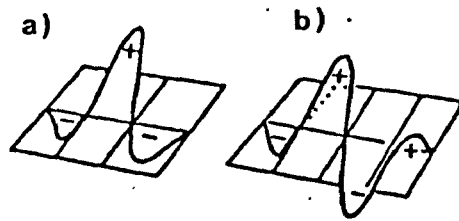


**Fig 2**  
Observed intensity shape resulting from  $C_L$  and  $C_D$  responses  
of an object of finite width. Zero crossings marked with arrows.





Schematic diagram of the receptive fields of simple cells in the visual cortex: (a) line detector, (b) edge detector

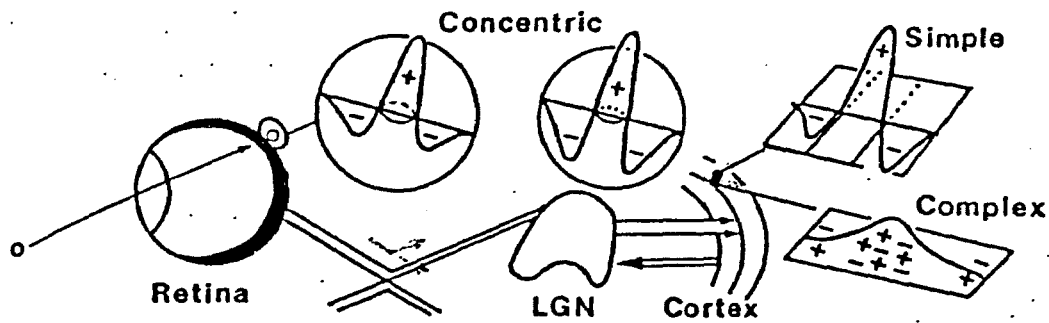


Fig 3a (Kulikowski, 1979)

Schematic diagram of the main visual pathways from retina to occipital cortex, showing the response profiles of receptive fields at various points along the pathway (positive to light spots, negative to dark spots). Also a separate diagram of the receptive fields of simple cells in the visual cortex: (a) line detector, (b) edge detector

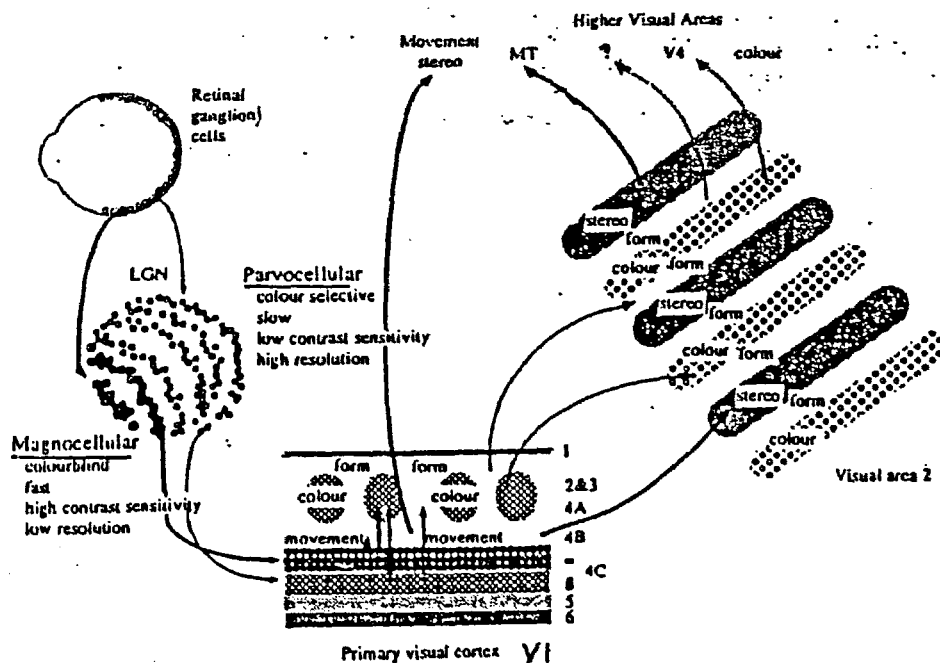


Fig 3b (Milner and Goodale, 1995)  
Magno and Parvo Paths from LGN to V1 laminae

# STOP!

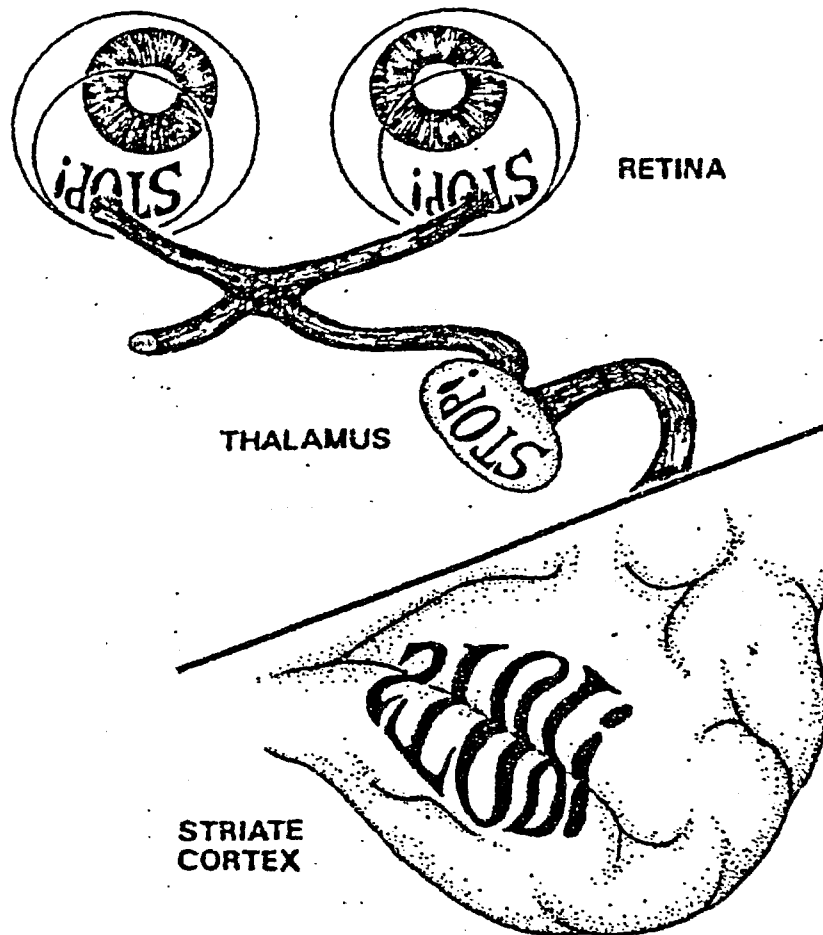
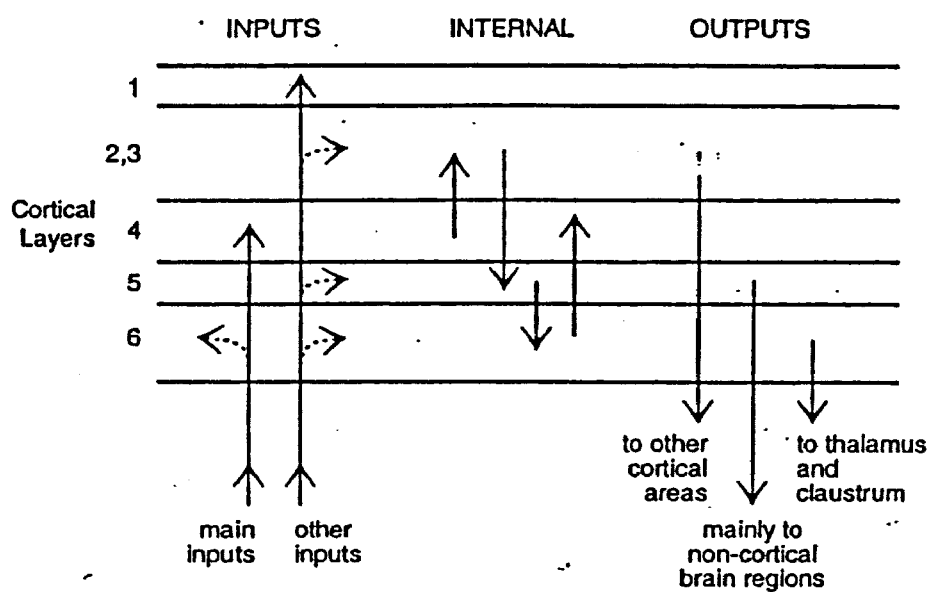


Fig 4 (Cook, 1986)

#### The Primary 'Retinotopic' Map

In the visual system, the retinal image in the eye maintains its basic configuration as the pattern of stimulation is transferred from the retina to the lateral geniculate body in the thalamus to striate cortex. In the human brain, the central one or two degrees of the visual field (5 – 10 mm wide at a reading distance of 45 cm) is represented bilaterally.



**Fig 5 (Crick, 1994)**  
**A grossly simplified diagram showing some of the major pathways within cortical area V1. There are many sideways connections that are not shown in this diagram.**